frontiers in Molecular Neuroscience

ORIGINAL RESEARCH
published: 30 January 2018
doi: 10.3389/fnmol.2018.00011

Inverse Modulation of Neuronal $K_V12.1$ and $K_V11.1$ Channels by 4-Aminopyridine and NS1643

Marlen Dierich[1†], Saskia Evers[1†], Bettina U. Wilke[1] and Michael G. Leitner[1,2]*

[1] *Department of Neurophysiology, Institute of Physiology and Pathophysiology, Philipps University of Marburg, Marburg, Germany,* [2] *Division of Physiology, Department of Physiology and Medical Physics, Innsbruck Medical University, Innsbruck, Austria*

The three members of the *ether-à-go-go-gene*-like (Elk; $K_V12.1$-$K_V12.3$) family of voltage-gated K^+ channels are predominantly expressed in neurons, but only little information is available on their physiological relevance. It was shown that $K_V12.2$ channels modulate excitability of hippocampal neurons, but no native current could be attributed to $K_V12.1$ and $K_V12.3$ subunits yet. This may appear somewhat surprising, given high expression of their mRNA transcripts in several brain areas. Native K_V12 currents may have been overlooked so far due to limited knowledge on their biophysical properties and lack of specific pharmacology. Except for $K_V12.2$, appropriate genetically modified mouse models have not been described; therefore, identification of K_V12-mediated currents in native cell types must rely on characterization of unique properties of the channels. We focused on recombinant human $K_V12.1$ to identify distinct properties of these channels. We found that $K_V12.1$ channels exhibited significant mode shift of activation, i.e., stabilization of the voltage sensor domain in a "relaxed" open state after prolonged channel activation. This mode shift manifested by a slowing of deactivation and, most prominently, a significant shift of voltage dependence to hyperpolarized potentials. In contrast to related $K_V11.1$, mode shift was not sensitive to extracellular Na^+, which allowed for discrimination between these isoforms. Sensitivity of $K_V12.1$ and $K_V11.1$ to the broad-spectrum K^+ antagonist 4-aminopyridine was similar. However, 4-AP strongly activated $K_V12.1$ channels, but it was an inhibitor of K_V11 channels. Interestingly, the agonist of K_V11 channels NS1643 also differentially modulated the activity of these channels, i.e., NS1643 activated $K_V11.1$, but strongly inhibited $K_V12.1$ channels. Thus, these closely related channels are distinguished by inverse pharmacological profiles. In summary, we identified unique biophysical and pharmacological properties of $K_V12.1$ channels and established straightforward experimental protocols to characterize $K_V12.1$-mediated currents. Identification of currents in native cell types with mode shift that are activated through 4-AP and inhibited by NS1643 can provide strong evidence for contribution of $K_V12.1$ to whole cell currents.

Keywords: K_V10, K_V11, K_V12, HERG, mode shift, voltage-dependent potentiation, 4-aminopyridine, NS1643

OPEN ACCESS

Edited by:
Alexandre Mourot, Université Pierre et Marie Curie, France

Reviewed by:
Marco Martina, Northwestern University, United States
Norelle Christine Wildburger, Washington University in St. Louis, United States

****Correspondence:***
Michael G. Leitner
Michael.Leitner@i-med.ac.at

[†] These authors have contributed equally to this work.

Received: *10 November 2017*
Accepted: *09 January 2018*
Published: *30 January 2018*

Citation:
Dierich M, Evers S, Wilke BU and Leitner MG (2018) Inverse Modulation of Neuronal $K_V12.1$ and $K_V11.1$ Channels by 4-Aminopyridine and NS1643. Front. Mol. Neurosci. 11:11. doi: 10.3389/fnmol.2018.00011

INTRODUCTION

The ether-à-go-go (Eag) superfamily of voltage-gated K^+ channels comprises three evolutionary conserved families that share high sequence homology: Ether-à-go-go (Eag; K_v10), ether-à-go-go-related-gene (Erg; K_v11) and ether-à-go-go-gene-like (Elk; K_v12) channels (Bauer and Schwarz, 2001). The best-studied member, $K_v11.1$ (the human isoform is referred to as HERG channel) mediates rapidly activating K^+ current I_{Kr} in cardiac myocytes determining heart action potential duration (Sanguinetti et al., 1995). Accordingly, loss of $K_v11.1$ channel function through mutations or drug treatment causes cardiac arrhythmia and sudden death in humans (Curran et al., 1995; Sanguinetti et al., 1995; Trudeau et al., 1995). K_v11 channels also mediate important K^+ currents in neurons of the auditory brainstem (Hardman and Forsythe, 2009), the olfactory bulb (Hirdes et al., 2009) and the midbrain (Ji et al., 2012). $K_v10.1$ channels regulate cell cycle progression and proliferation (Sanchez et al., 2016; Urrego et al., 2016), and are frequently overexpressed in human cancers with poor prognosis (Pardo and Stuhmer, 2014). $K_v10.1$ channel mutations cause developmental disorders and epilepsy (Kortum et al., 2015; Simons et al., 2015).

In contrast to K_v10 and K_v11 channels, only little information on physiological relevance is available for the three members of the K_v12 family that are expressed predominantly in neurons (Engeland et al., 1998; Shi et al., 1998; Miyake et al., 1999; Trudeau et al., 1999; Saganich et al., 2001; Zou et al., 2003). $K_v12.2$ channels regulate excitability in pyramidal neurons of hippocampus in mice (Zhang et al., 2010), but no native current component could be attributed to $K_v12.1$ and $K_v12.3$ subunits despite expression of their mRNA transcripts in several brain areas (Shi et al., 1998; Miyake et al., 1999; Saganich et al., 2001; Zou et al., 2003). We consider that $K_v12.1$/$K_v12.3$-mediated currents in neurons were overlooked so far due to insufficient knowledge on biophysical properties and lack of specific pharmacological tools.

Recently, it was shown that $K_v12.1$ channels exhibit mode shift of activation (also termed pre-pulse facilitation or voltage-dependent potentiation) (Li et al., 2015; Dai and Zagotta, 2017). Mode shift denotes time-dependent stabilization of the voltage sensor domain in a "relaxed" open state after prolonged channel activation through depolarized (conditioning) membrane potentials (Bezanilla et al., 1982; Villalba-Galea et al., 2008). It manifests by slowing of deactivation and a shift of voltage dependence to hyperpolarized potentials (Li et al., 2015; Dai and Zagotta, 2017). Accordingly, when measured with routine voltage clamp protocols (e.g., holding potentials of −60 mV) human $K_v12.1$ channels mediate "conventional" K^+ currents that activate similar to many other K_v channels with voltages at half-maximal activation of around −30 mV (c.f. **Figure 1**) (Li et al., 2015). These currents could easily go unnoticed in cell types expressing different endogenous K^+ currents. Taking into account their mode shift, appropriate voltage protocols (e.g., depolarized holding potentials) may uncover K_v12-mediated currents. However, it remains to be explored whether mode shift can be detected in cells expressing various K^+ currents and whether it may be employed to identify native $K_v12.1$ channels. Mode shift is not an exclusive feature of $K_v12.1$ channels, but has been demonstrated also for voltage-gated Na^+ channels (Bezanilla et al., 1982), HCN (Mannikko et al., 2005; Bruening-Wright and Larsson, 2007), *Shaker* (Olcese et al., 1997; Tilegenova et al., 2017), and $K_v11.1$ (Erg1) channels (Piper et al., 2003; Tan et al., 2012; Goodchild et al., 2015). Nevertheless, it may constitute a prominent hallmark to distinguish K_v12 channels from other K^+ current components in native tissue.

Here we describe biophysical and pharmacological properties of $K_v12.1$ channels and demonstrate straightforward experimental protocols that may be employed to identify K_v12 currents in neurons. We show, that these properties allowed detection of $K_v12.1$-mediated currents in cells expressing a variety of different K^+ channels. Our findings may be utilized to identify physiological roles of $K_v12.1$ channels.

RESULTS

Voltage-Dependent Mode Shift of Human $K_v12.1$ Channels

Mode shift of human $K_v12.1$ channels was recently demonstrated (Li et al., 2015), but a detailed characterization is currently not available. In order to identify exclusive properties of human $K_v12.1$ channels, we thus set out with detailed biophysical analysis of these channels in an overexpression system. In CHO cells, activation of $K_v12.1$ channels through depolarizing voltage steps produced robust outwardly rectifying currents (**Figure 1A**) (Zou et al., 2003; Li et al., 2015; Dai and Zagotta, 2017). Channel deactivation at hyperpolarized potentials was best described by double exponential kinetics, and deactivation slowed down with more depolarized pre-potentials (**Figures 1B,C**). When we activated $K_v12.1$ channels at 0 mV for different time intervals, tail current amplitudes increased (**Figures 1D,E**) and deactivation slowed down with the duration of the pre-pulse (**Figure 1F**). Tail current increase and slowing of deactivation saturated at a pulse duration of about 200 ms and 400–500 ms, respectively.

We then analyzed voltage dependence of human $K_v12.1$ channels with voltage protocols established previously to study mode shift of related $K_v11.1$ (Tan et al., 2012). We applied depolarizing holding potentials (conditioning potentials; 200 ms) before a series of activating voltage steps (pulse potentials from −140 mV to +10 mV; 600 ms) (**Figure 1G** and Supplementary Figures 1A–C). To minimize time intervals at hyperpolarized potentials that may counteract mode shift (c.f. Villalba-Galea, 2017), we at start recorded tail currents at correspondingly depolarized potentials (**Figures 1G–I**). In these experiments, amplitudes of $K_v12.1$-mediated outward currents were similar irrespective of conditioning potentials. This indicated that comparable steady-state channel activation was reached with all voltage protocols (Supplementary Figures 1A–C). After a conditioning potential of −60 mV, voltage dependence of $K_v12.1$ channels also did not change relevantly upon extension of the activating steps to 4000 ms (**Figures 1J,K**). This additionally demonstrated that steady-state activation of $K_v12.1$ channels was already reached by activating pulses as short as 600 ms.

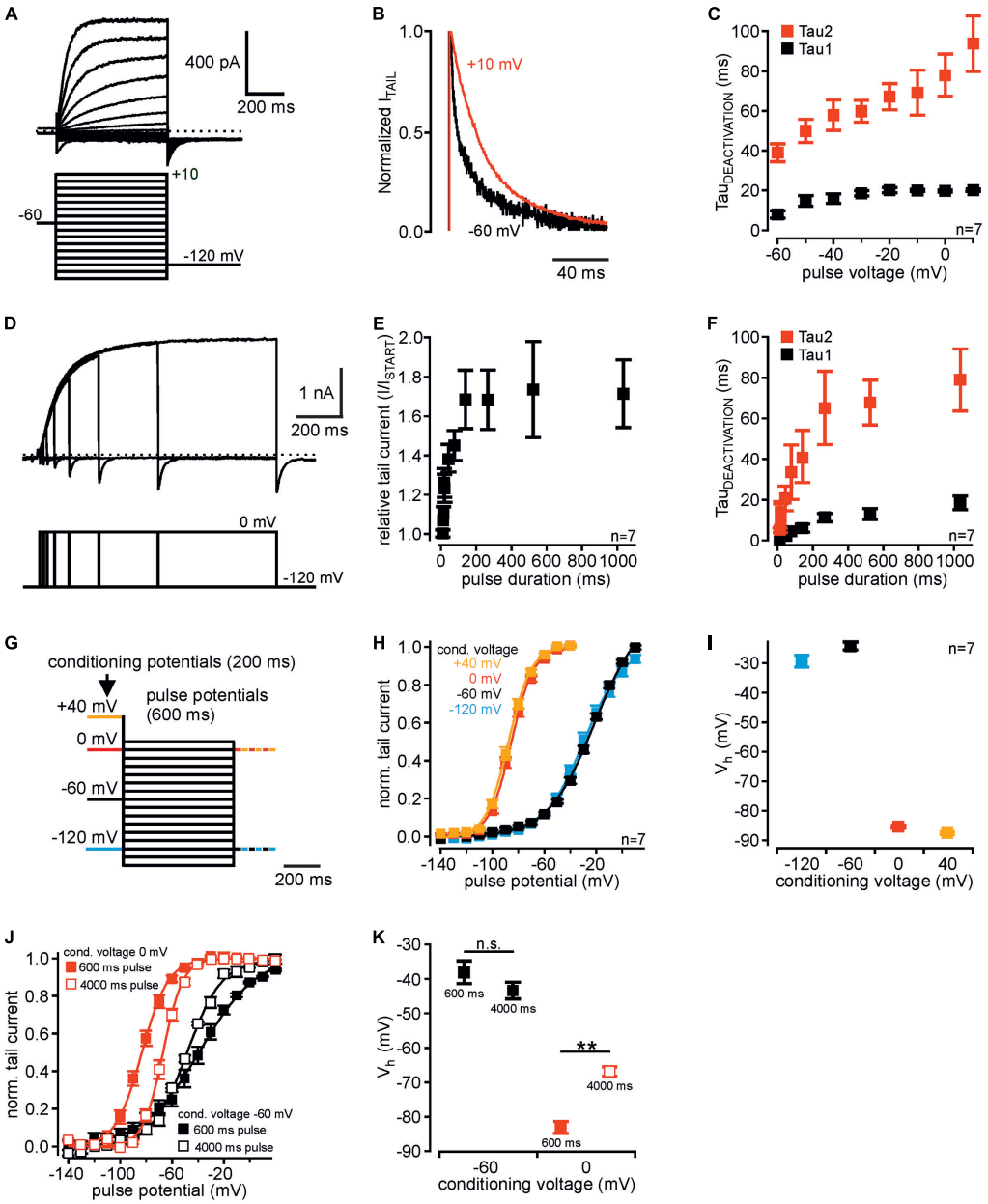

FIGURE 1 | Voltage-dependent mode shift of human $K_v12.1$ channels. **(A)** Representative patch clamp recording of a CHO cell transiently transfected with human $K_v12.1$ channels measured with the indicated voltage protocol. **(B)** Representative tail currents elicited at –120 mV after activating pulses of –60 mV (black) and +10 mV (red). Currents were normalized to maximum amplitude for visualization of deactivation kinetics (currents from recording shown in **A**). **(C)** Tail current deactivation was best described by double exponential kinetics: Tau1 and tau2 were derived from double-exponential fits to the decaying phase of tail currents (voltage protocols as in **A**). Deactivation slowed down with channel activation at more depolarized potentials. **(D–F)** When $K_v12.1$ channels were activated at 0 mV for different time intervals, **(E)** tail current amplitudes increased and **(F)** deactivation slowed-down with pre-pulse duration. Tail current increase and slowing of deactivation saturated at a pulse duration of about 200 ms and 400–500 ms, respectively (**D** shows a representative recording). **(G–I)** Analysis of voltage dependence of recombinant $K_v12.1$ channels. **(G)** Voltage protocols consisted of a 200 ms conditioning potential step to –120 mV (blue), –60 mV (black), 0 mV (red), or +40 mV (orange), followed by 600 ms activating pulse potentials from –140 to +10 mV (10 mV increments). In these experiments, tail currents were elicited either at –120 mV or at 0 mV (for representative recordings see Supplementary Figures 1A,C). **(H)** Summary of voltage dependence of human $K_v12.1$ channels derived from Boltzmann fits to individual recordings as shown in Supplementary Figures 1A,C (solid line represents a Boltzmann fit to averaged data). Depolarized conditioning potentials of +40 and 0 mV induced a large shift of voltage dependence to hyperpolarized potentials. **(I)** shows mean V_h of channel activation in dependence of conditioning potentials (derived from fits shown in **H**). **(J,K)** Upon extension of the activating pulses from 600 ms (filled black squares) to 4000 ms (open black squares), voltage dependence of recombinant $K_v12.1$ channels was not significantly changed when measured after a conditioning pulse of –60 mV. However, extension of the activating pulse to 4000 ms significantly shifted voltage dependence of $K_v12.1$ channels to depolarized potentials after conditioning voltage of 0 mV ($P \leq 0.01$; open red squares). For data shown in **(J)** eight independent recordings were averaged (each cell measured with all four voltage protocols). There was no significant difference between corresponding data in **(J,K)** and **(H,I)** (conditioning potential –60 mV, 600 ms).

For 600 ms activating pulses, half-maximal voltages of activation (V_h) were −29.3 ± 2.3 mV and −24.1 ± 1.6 mV for negative conditioning potentials of −120 mV or −60 mV, respectively (n = 7; 600 ms activating pulses; **Figures 1H,I**). When cells were held at depolarized conditioning pulses of 0 mV or +40 mV, V_h was −85.3 ± 0.9 mV and −87.6 ± 0.8 mV, respectively (**Figures 1H,I**; 600 ms activating pulses). In these experiments, slope factors derived from Boltzmann fits to the recordings changed from −15.7 ± 0.7 mV (conditioning pulse of −120 mV) and −16.4 ± 0.9 mV (−60 mV) to −8.6 ± 0.1 mV (0 mV) and −8.9 ± 0.6 (+40 mV) (n = 7; Supplementary Figure 1D; 600 ms activating pulses). Accordingly, depolarizing conditioning potentials induced a large shift of voltage dependence by about −60 mV, and the full shift occurred across a potential range of 60 mV (between holding potentials of −60 and 0 mV). In analogous experiments, the same conditioning voltages shifted V_h of related $K_v11.1$ channels from −6.8 ± 4.4 mV (conditioning voltage −60 mV) to −62.4 ± 1.5 (conditioning voltage +40 mV; n = 7; **Figures 2A,B**), consistent with a previous report (Tan et al., 2012).

We next tested whether mode shift was sensitive to the employed voltage protocol. Therefore, we again applied 200 ms depolarized conditioning pulses, but this time we extended the activating pulses to 4000 ms (**Figures 1J,K**). When in these experiments cells were held at conditioning pulses of −60 and 0 mV, V_h was −43.3 ± 2.5 mV and −66.8 ± 1.5 mV, respectively (**Figures 1J,K**). Thus, mode shift of $K_v12.1$ channels was readily induced also when activating the channels for 4000 ms. However, the extent of mode shift was significantly reduced in these experiments compared to experiments with 600 ms activating pulses (**Figure 1K**; $P \geq 0.01$), i.e., increased time intervals at hyperpolarized holding potentials during these protocols presumably counteracted development of mode shift. Similarly, the extent of mode shift was reduced when we activated channels for 600 ms after conditioning pulses of −60 and 0 mV, but recorded tail currents at hyperpolarized holding potentials (−120 mV; Supplementary Figures 1E,F), i.e., we introduced additional hyperpolarizing potentials after every activating pulse. Thus, also in these experiments hyperpolarizing holding potentials between the conditioning pulses reduced the expression of mode shift.

Taken together, human $K_v12.1$ channels exhibited significant voltage-dependent mode shift that in response to depolarized holding potentials manifested by slowed channel deactivation and by a large hyperpolarizing shift of voltage dependence. This mode shift of $K_v12.1$ channels can be induced robustly employing different voltage protocols, but the extent of mode shift significantly varies with duration of hyperpolarized holding potentials.

In Contrast to $K_v11.1$, $K_v12.1$ Channels Are Insensitive to Extracellular Na^+

Inhibition of K_v11 channels by extracellular Na^+ is well established (Numaguchi et al., 2000; Sturm et al., 2005) and a hallmark used to identify K_v11-mediated currents in neurons (e.g., Hardman and Forsythe, 2009). In control experiments, replacement of extracellular Na^+ with NMDG without altering extracellular K^+ concentration slightly increased $K_v11.1$-mediated outward currents (**Figure 2A**), as previously reported (Numaguchi et al., 2000). Upon removal of extracellular Na^+, activation voltage range of $K_v11.1$ channels conditioned at −60 and +40 mV shifted to hyperpolarized potentials by −24.4 ± 1.5 mV and −13.9 ± 0.7 mV, respectively (n = 7; **Figures 2B,C**). Accordingly, overall mode shift of voltage dependence was attenuated from −55.7 ± 4.4 mV under control conditions to −45.1 ± 3.5 mV in absence of extracellular Na^+ (n = 7; $P \leq 0.05$). We then tested whether related $K_v12.1$ channels also exhibited such Na^+ sensitivity. We found that neither current amplitudes nor voltage dependence of $K_v12.1$ channels were affected by removal of extracellular Na^+ (**Figures 2D–F**). Consequently, the extent of mode shift was also insensitive to changes of the Na^+ concentration. To conclude, despite the high similarity in mode shift behavior, the absence of Na^+ sensitivity in $K_v12.1$ channels distinguishes $K_v11.1$-mediated currents from $K_v12.1$.

$K_v12.1$ Channels Are Not Sensitive to K_v Channel Blockers E-4031, XE991, and TEA

We then evaluated whether $K_v12.1$ channels were sensitive to channel inhibitors that are widely used to attribute neuronal K^+ currents to particular channel families. At concentrations generally applied to inhibit established target channels, human $K_v12.1$ channels were insensitive to both E-4031 (20 μM), a specific inhibitor of K_v11 channels (Supplementary Figures 2A,B) (Trudeau et al., 1995), and XE991 (10 μM), a specific antagonist of neuronal K_v7 (KCNQ) channels (Supplementary Figures 2D,E) (Wang et al., 1998). $K_v12.1$-mediated currents were also insensitive to E-4031 and XE991 concentrations up to 100 μM (Supplementary Figures 2C,F). $K_v12.1$ channels also were not affected by the broad-spectrum K^+ channel inhibitor tetraethylammonium (TEA) at a concentration that completely inhibited $K_v7.2$ channels (5 mM; Supplementary Figures 2G,H) (Hadley et al., 2000). However, $K_v12.1$ channels were slightly inhibited by 50 and 100 mM TEA ($I_{50mM\,TEA}/I_{Start}$ = 0.90 ± 0.01; $I_{100mM\,TEA}/I_{Start}$ = 0.83 ± 0.01; n = 9; Supplementary Figure 2I). Of note, low sensitivity of $K_v12.1$ channels to E-4031 and TEA has been shown in an early report (Shi et al., 1998). In summary, E-4031, XE991 and TEA cannot be used to inhibit $K_v12.1$ channels in native tissue, but may be used to isolate $K_v12.1$ channel activity through inhibition of other K^+ channels.

The Broad-Spectrum K^+ Channel Antagonist 4-Aminopyridine (4-AP) Activates $K_v12.1$

We then tested whether human $K_v12.1$ channels were sensitive to 4-AP, another established antagonist of several K_v families (Gutman et al., 2005). Surprisingly, 4-AP at a concentration well in the range often used to isolate neuronal K^+ currents (3 mM; e.g., Marcotti et al., 2003) increased $K_v12.1$-mediated steady-state and tail currents within seconds (**Figures 3A–C**). Current potentiation was the same for conditioning pulses of −60 and

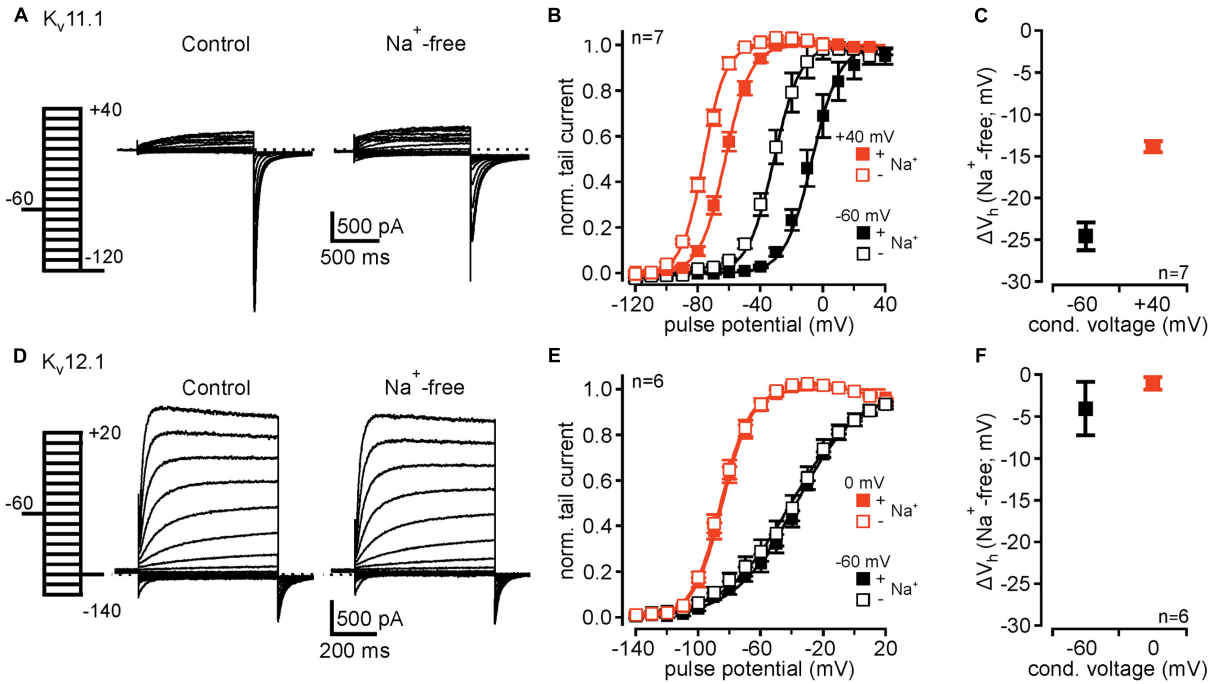

FIGURE 2 | $K_v12.1$ are not sensitive to extracellular Na^+. **(A)** Representative recordings from a CHO cell transiently transfected with $K_v11.1$ under control conditions (left) and after removal of external Na^+ (right). **(B)** $K_v11.1$ channels exhibit mode shift of activation, as previously reported. After conditioning potential of +40 mV voltage dependence of $K_v11.1$ channels shifted to hyperpolarized potentials, compared to conditional potential of –60 mV [solid lines represent a Boltzmann fit to averaged data; from recordings as shown in **(A)**]. Upon removal of extracellular Na^+, voltage dependence of $K_v11.1$ shifted to hyperpolarized potentials after conditioning potentials of –60 and +40 mV. **(C)** Shows averaged shifts of V_h (ΔV_h) for conditional potentials of –60 and +40 mV after removal of extracellular Na^+. **(D–F)** Recombinant $K_v12.1$ channels are insensitive to extracellular Na^+. **(D)** Representative recordings of $K_v12.1$-mediated currents under control conditions (left) and in absence of extracellular Na^+ (right). **(E)** Summary of voltage dependence of $K_v12.1$ channels derived from experiments presented in **(D)**. Note that neither current amplitudes nor voltage dependence of $K_v12.1$ channels were affected by removal of extracellular Na^+. **(F)** shows that removal of extracellular Na^+ did not shift V_h (ΔV_h) of activation of $K_v12.1$ channels. In these experiments, Na^+ in the extracellular solution was replaced by NMDG without changing extracellular K^+ concentration.

0 mV, and 4-AP potentiated currents at all holding potentials positive to −60 mV (**Figure 3C**). 4-AP-dependent current increase was reversible within 2–3 min after washout of the drug (**Figure 3D**). 4-AP (3 mM) not only potentiated $K_v12.1$-mediated currents, but also significantly shifted the voltage dependence of $K_v12.1$ channels to hyperpolarized potentials (**Figure 3E**). Compared to control recordings measured before application of the substance, 3 mM 4-AP shifted V_h by -19.7 ± 1.7 mV ($n = 7$; $P \leq 0.001$) and by -10.4 ± 1.5 mV ($n = 7$; $P \leq 0.001$) after condition voltage pulses of −60 and 0 mV, respectively. Thus, the shift of V_h was significantly more pronounced for currents conditioned at −60 mV ($P \leq 0.01$; c.f. **Figure 3E**).

We then analyzed the dose-response relationship of 4-AP action on $K_v12.1$ channels. As 5 and 10 mM 4-AP increased pH of the solution to about 8.1 and 9.0, respectively, we adjusted pH of these solutions to 7.4 after addition of 4-AP. Of note, 3 mM 4-AP or lower 4-AP concentrations did not alter the pH of the solution relevantly and thus no adjustment of pH was necessary. Under these experimental conditions, 4-AP potentiated $K_v12.1$ currents in a concentration-dependent manner with an EC_{50} of about 2.1 and a Hill coefficient of about 0.8 (**Figure 3F**, *red trace*). In contrast, $K_v11.1$ channels were inhibited by 4-AP with an IC_{50} of approximately 2.6 mM and a Hill coefficient of about 0.7 (Supplementary Figure 3), consistent with previous reports (e.g., Ridley et al., 2003). Thus, despite inverse effects of 4-AP on $K_v12.1$ and $K_v11.1$, the sensitivity of both channels to 4-AP was quite similar. When we applied 5 mM or 10 mM 4-AP without adjusting pH, we found that these concentrations activated $K_v12.1$ channel even stronger than at physiological pH (**Figures 3F,G**). Without adjusting pH at higher concentrations, the EC_{50} was about 3.1 and the Hill coefficient was 0.9 (**Figure 3F**, *black trace*). As in line with a previous study (Kazmierczak et al., 2013) increasing pH of the extracellular solution from 7.4 to 8.1 or 9.0 without addition of 4-AP did not potentiate $K_v12.1$-mediated steady-state currents (**Figure 3G**), these data suggested that 4-AP activated $K_v12.1$ channels more efficiently at more alkaline pH. Indeed, increasing pH of the extracellular solution containing 3 mM 4-AP to 8.1 further increased $K_v12.1$-mediated steady-state outward currents (**Figure 3H**).

$K_v12.1$ Channels Are Also Activated by Isomeric Aminopyridines

Several other aminopyridines have been shown to inhibit voltage-gated K^+ channels, albeit antagonistic efficiency of these substances was lower than that of 4-AP (Robertson

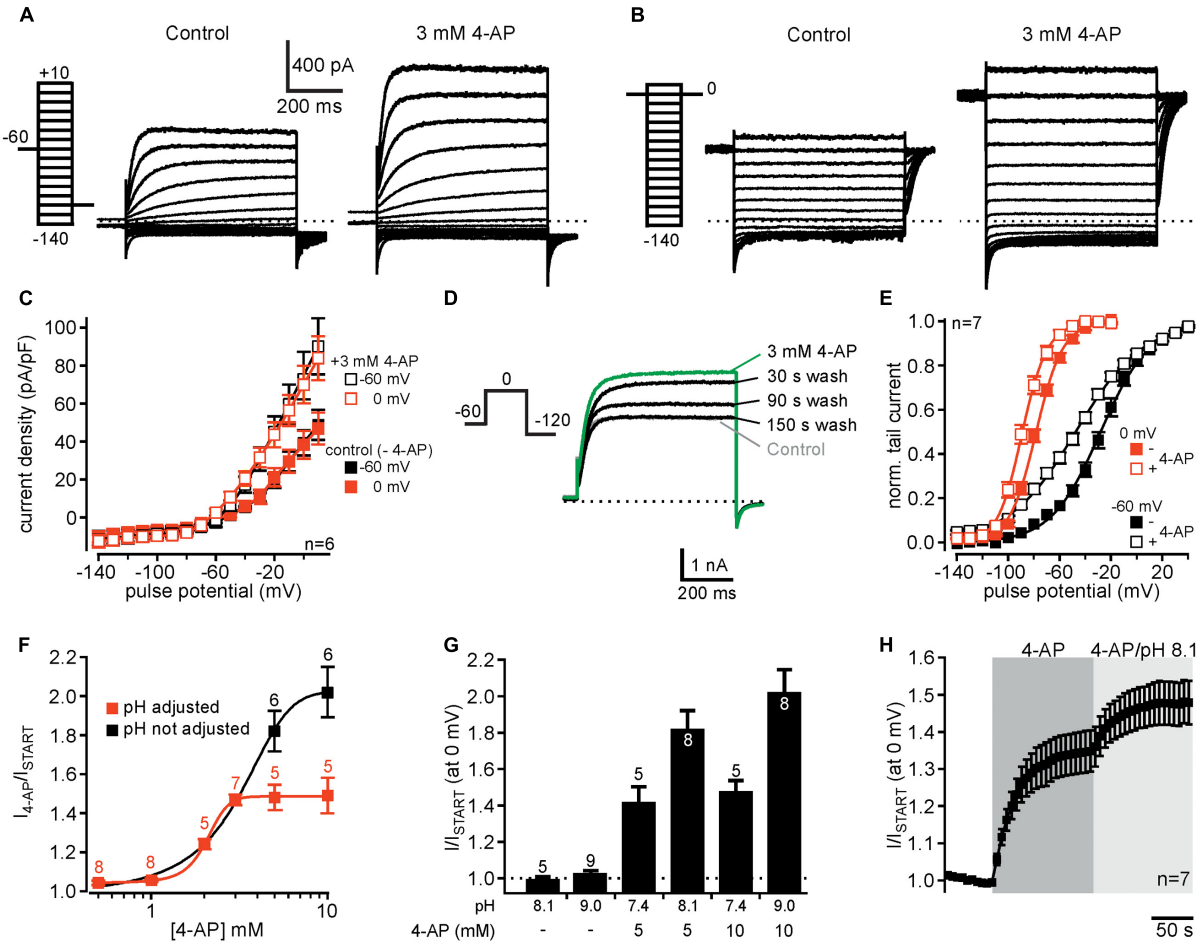

FIGURE 3 | 4-AP potentiates currents through human $K_v12.1$ channels. **(A,B)** Representative recordings from a CHO cell transiently transfected with $K_v12.1$ before (left) and after extracellular application of 3 mM 4-AP (right) after conditioning pulses of **(A)** –60 mV and **(B)** 0 mV. **(C)** 4-AP-dependent activation of $K_v12.1$-mediated steady-state outward currents was independent on employed voltage protocols (summary of recordings as presented in **A,B**). 4-AP potentiated currents at all holding potentials positive to –60 mV. **(D)** 4-AP-dependent potentiation of $K_v12.1$ currents was reversible, as current amplitudes returned to control levels within 2–3 min after removal of the substance [shown are representative recordings under control conditions (gray), after application of 3 mM 4-AP (green) and at different time points (30, 90, and 150 s) after washout of 4-AP]. **(E)** 3 mM 4-AP shifted the voltage dependence of human $K_v12.1$ channels to hyperpolarized potentials (open squares) [the panel shows Boltzmann fits to averaged data; data obtained from recordings as shown in **(A,B)**]. **(F)** 4-AP activated $K_v12.1$ channels in a dose-dependent manner. When pH of the extracellular solution was adjusted to 7.4 at higher 4-AP concentrations, the EC_{50} was about 2.1 mM and the Hill coefficient was about 0.8 (red trace). When pH of the solutions was not adjusted, the EC_{50} was about 3.1 and Hill coefficient was 0.9 (black trace). Parameters were derived from fits of averaged data to a Hill equation described in Section "Materials and Methods" (solid line represents fit; note that addition of 4-AP to 5 and 10 mM 4-AP increased the pH of the solution to 8.1 and 9.0, respectively). **(G)** Increasing the pH of the extracellular solution from 7.4 to 8.1 or 9.0 without addition of 4-AP did not increase $K_v12.1$-mediated steady-state currents. In contrast, application of 5 mM or 10 mM 4-AP in extracellular solution without adjusting pH activated $K_v12.1$ channels even more strongly than when pH of the solution was adjusted to pH 7.4. **(H)** Application of 3 mM 4-AP that does not change pH of the extracellular solution strongly potentiated $K_v12.1$-mediated currents. Current potentiation through 3 mM 4-AP was further increased when the pH of the extracellular solution was increased to pH 8.1.

and Nelson, 1994; Sedehizadeh et al., 2012; Strupp et al., 2017). We thus wondered whether we could identify isomeric aminopyridines that activated $K_v12.1$, at best without affecting other K^+ channels. We found that 2-aminopyridine (2-AP) and 3-aminopyridine (3-AP) potentiated $K_v12.1$-mediated currents at a concentration close to the EC_{50} of 4-AP (3 mM) by about 20% ($P \leq 0.001$) and 7% ($P \leq 0.001$), respectively (**Figure 4**). At the same concentration 3,4-diaminopyridine (3,4-DAP; 3 mM) was ineffective. Hence, 2-AP ($P \leq 0.01$) and 3-AP ($P \leq 0.001$) activated $K_v12.1$ channels significantly less than 4-AP mirroring efficacy of inhibition of other K^+ channels by these substances (Robertson and Nelson, 1994; Sedehizadeh et al., 2012; Strupp et al., 2017).

NS1643, an Activator of K_v11 Channels, Inhibits $K_v12.1$ Channels

We then turned to NS1643, a partial agonist of the K_v11 channel family (Casis et al., 2006). As shown earlier (c.f. Hansen et al., 2006), NS1643 (30 μM) slowed channel deactivation and

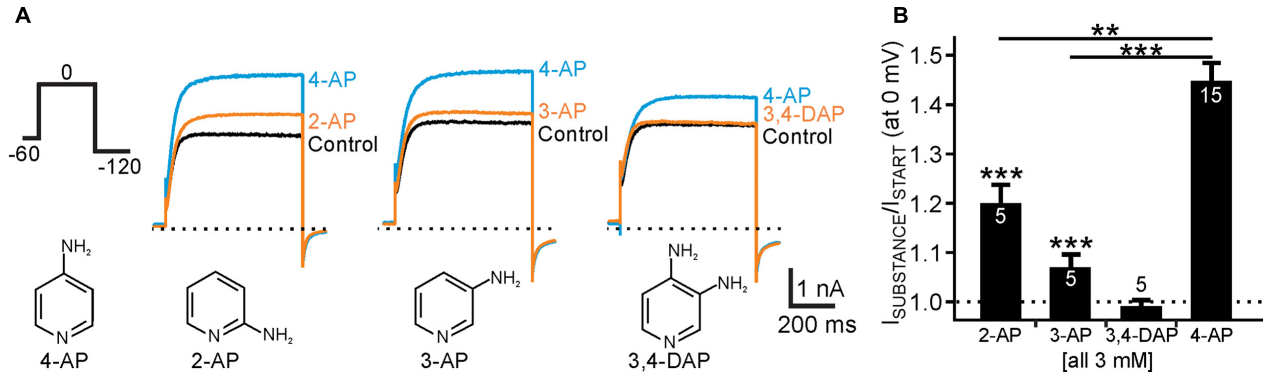

FIGURE 4 | Activation of human K_v12.1 channels by isomeric aminopyridines. **(A)** Representative whole cell currents through human K_v12.1 channels elicited by voltage steps to 0 mV (voltage protocol as indicated). The upper panel shows effects of 2-AP (left), 3-AP (middle), or 3,4-DAP (right) on human K_v12.1 channels. 4-AP was applied at the end of every recording for comparison of current potentiation (concentration of all substances was 3 mM). The lower panel displays chemical structures of 4-AP, 2-AP, 3-AP, and 3,4-DAP. **(B)** Summary of recordings as presented in **A** (steady-state outward currents at 0 mV were analyzed at the end of the activating pulse). At the same concentration (all 3 mM), 2-AP and 3-AP significantly potentiated K_v12.1-mediated currents, albeit to a lower extent than 4-AP (**$P \leq 0.01$; ***$P \leq 0.001$).

potentiated K_v11.1-mediated outward currents (**Figures 5A–C**). In contrast, the same concentration of NS1643 (30 μM) completely inhibited K_v12.1 channels with a time constant of 16.8 ± 2.6 s (n = 7; **Figures 5A–C**). When we applied only 10 μM NS1643, a concentration close to the reported EC_{50} of NS1643 for activation of K_v11.1 channels (Casis et al., 2006), K_v12.1-mediated currents were reduced to 37.1 ± 4.1% of initial current amplitudes. Inhibition of currents by 10 μM was much slower than when 30 μM NS1643 was applied (n = 6; compare **Figure 5B** and Supplementary Figure 4). We then analyzed voltage dependence of residual K_v12.1 currents in the presence of 10 μM NS1643 (**Figures 5D–F**): Application of NS1643 (10 μM) shifted V_h by +8.8 ± 2.9 mV (n = 6; $P \leq 0.05$) and by +21.7 ± 5.2 mV (n = 6; $P \leq 0.01$) after condition voltage pulses of −60 and 0 mV, respectively (**Figures 5D–F**). At the same time, slope factors changed by +8.0 ± 1.5 mV (conditioning pulse of −60 mV; n = 6; $P \leq 0.05$) and −1.8 ± 0.9 mV (conditioning pulse 0 mV; n = 6; $P \leq 0.01$). Furthermore, NS1643 (10 μM) significantly accelerated deactivation of K_v12.1 channels at hyperpolarized potentials (**Figures 5G,H**; $P \leq 0.05$; n = 6).

Identification of K_v12.1 Currents in Cells Expressing Different K^+ Currents

Our results suggested that voltage-clamp protocols designed to detect mode shift in combination with pharmacology using 4-AP or NS1643 should provide a robust approach for isolation of K_v12.1-mediated currents in native cell types. As proof of principle, we sought to isolate K_v12.1 channel activity in cells expressing different K^+ channels (**Figure 6**). To this end, we co-expressed K_v12.1 channels together with K_v11.1 and typical neuronal K^+ channels (K_v7.2, K_v7.3 and Kir2.1). In these experiments, CHO cells were transiently transfected with equal amounts of plasmid DNA encoding the channel subunits (see section "Materials and Methods" for details). We first analyzed whether we could isolate Kir2.1- and K_v7-mediated currents in those cells. In all cells tested, we found large inward currents at hyperpolarized potentials and XE991-sensitive outward currents at depolarized potentials demonstrating expression of functional Kir2.1 and K_v7 channels, respectively (Supplementary Figure 5). As measure for abundance of K_v11.1 and K_v12.1 channels, we then tested whether we could detect mode shift of voltage dependence in the mix of K^+ currents. As determined from whole cell currents, V_h was −6.7 ± 1.3 mV and −80.0 ± 2.1 mV after conditioning potentials of −60 and 0 mV, respectively (n = 7; **Figures 6A–C**). Thus, mode shift of channels expressed in these cells (K_v11.1 and K_v12.1 channels) was readily detectable even among a complement of different voltage-dependent K^+ channels. We next attempted to isolate K_v12.1-mediated currents among the mixture of K^+ channel by making use of the pharmacological profile established above. 4-AP (3 mM) shifted the voltage dependence of whole cell currents by −8.5 ± 0.9 mV (n = 7; $P \leq 0.001$) and by −12.3 ± 2.3 mV (n = 7; $P \leq 0.05$) to hyperpolarized potentials after conditioning voltages of −60 and 0 mV, respectively (**Figures 6B,C**). Thus, although being less pronounced than for K_v12.1 channels alone (**Figure 6C**), the 4-AP-induced shift of voltage dependence was readily detectable in the mixed K^+ current situation. At the same time, 4-AP (3 mM) potentiated whole cell currents elicited at −60 and 0 mV to about 210% and 140% of baseline amplitudes, respectively (**Figures 6A,D–F**). Finally, we applied 30 μM NS1643 (on top of 4-AP) to the same cells and found that the substance inhibited outward currents and inward tail currents (**Figures 6A,D,E**). NS1643 also slowed deactivation kinetics of remaining currents (c.f. **Figure 6A**) indicating that NS1643-sensitive and functional K_v11.1 channels were expressed in these cells.

Taken together, using abovementioned experimental protocols we could unequivocally identify properties of K_v12.1 channels (mode shift, 4-AP and NS1643 sensitivity) among a mixture of K^+ currents. These results therefore suggest that the same protocols may be used to assign K^+ current components to K_v12.1 channels in complex (native) cellular/neuronal settings.

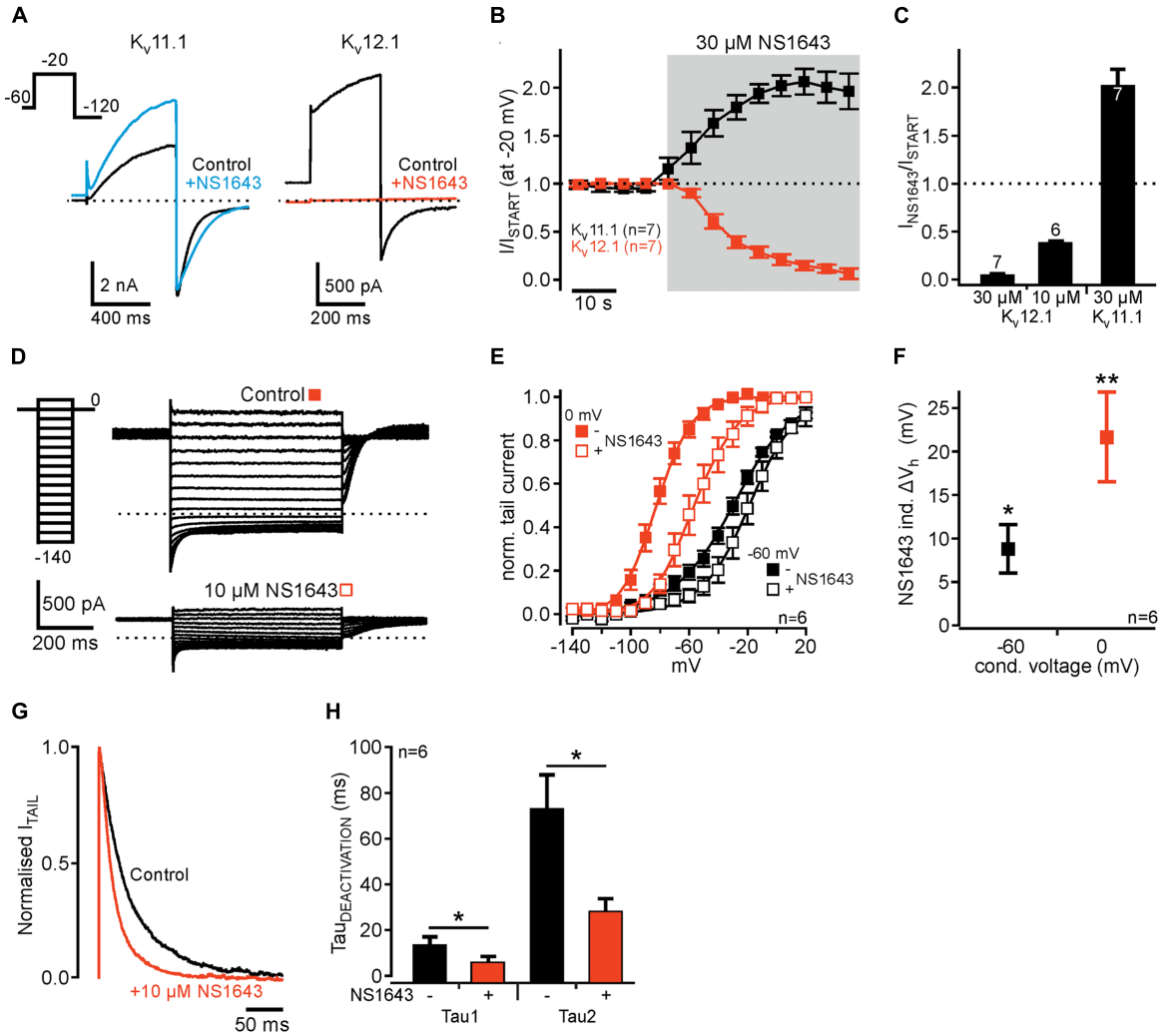

FIGURE 5 | Human $K_v12.1$ channels are inhibited by NS1643. **(A)** Representative recordings of recombinant $K_v11.1$ (left) and $K_v12.1$ (right) channels before (black) and after (colored) application of 30 µM NS1643 (voltage protocol as indicated). **(B)** Averaged time course of the amplitudes of outward currents mediated by $K_v11.1$ (black) and $K_v12.1$ (red) channels upon application of 30 µM NS1643. NS1643 activated $K_v11.1$ channels [as previously reported; (Casis et al., 2006; Hansen et al., 2006)], but completely inhibited $K_v12.1$ channels (data were derived from recordings as in **A**). **(C)** Summarized effects of NS1643 on $K_v11.1$ and $K_v12.1$ channels. 10 µM NS1643 did not completely inhibit $K_v12.1$ channels allowing for further analysis of remaining currents. The time course of $K_v12.1$ current inhibition by 10 µM NS1643 is shown in Supplementary Figure 4. **(D–F)** Voltage dependence of $K_v12.1$ channels changes through application of 10 µM NS1643. **(D)** Representative recordings of $K_v12.1$ channels after conditioning potential of 0 mV before (top) and after (bottom) application of 10 µM NS1643 (for clarity only these recordings are shown). **(E)** 10 µM NS1643 significantly shifted voltage dependence of $K_v12.1$ channels to depolarized potentials (solid lines represent Boltzmann fits to averaged data). **(F)** Shows averaged shifts of V_h (ΔV_h) induced by 10 µM NS1643 for currents conditioned at –60 and 0 mV. **(G,H)** NS1643 significantly accelerated $K_v12.1$ channel deactivation. **(G)** Representative normalized tail currents elicited at –120 mV after activation at –20 mV before (control, black) and after (red) application of 10 µM NS1643. **(H)** Shows averaged time constants of deactivation before and after application of NS1643 (10 µM) (*$P \leq 0.05$; **$P \leq 0.01$).

DISCUSSION

The three members of the *ether-à-go-go*-like channel family of voltage-gated K^+ channels ($K_v12.1$-$K_v12.3$) are predominantly expressed in neurons, as shown by mRNA transcripts in several brain areas including cerebral cortex and hippocampus (Miyake et al., 1999; Trudeau et al., 1999; Saganich et al., 2001; Zou et al., 2003), as well as in sympathetic ganglia (Shi et al., 1998). However, neuronal current components and their physiological relevance have been resolved for $K_v12.2$ subunits exclusively: as demonstrated by application of a selective inhibitor, $K_v12.2$ activity controls resting membrane potential and spontaneous firing of pyramidal neurons in hippocampus (Zhang et al., 2010). Also, in $K_v12.2$ knock-out mice it was shown that $K_v12.2$ channels regulate hippocampal excitability (Zhang et al., 2010) and may be important for processing of spatial working memory (Miyake et al., 2009). However, it is not known whether K_v12 channels mediate relevant currents in any other physiological system.

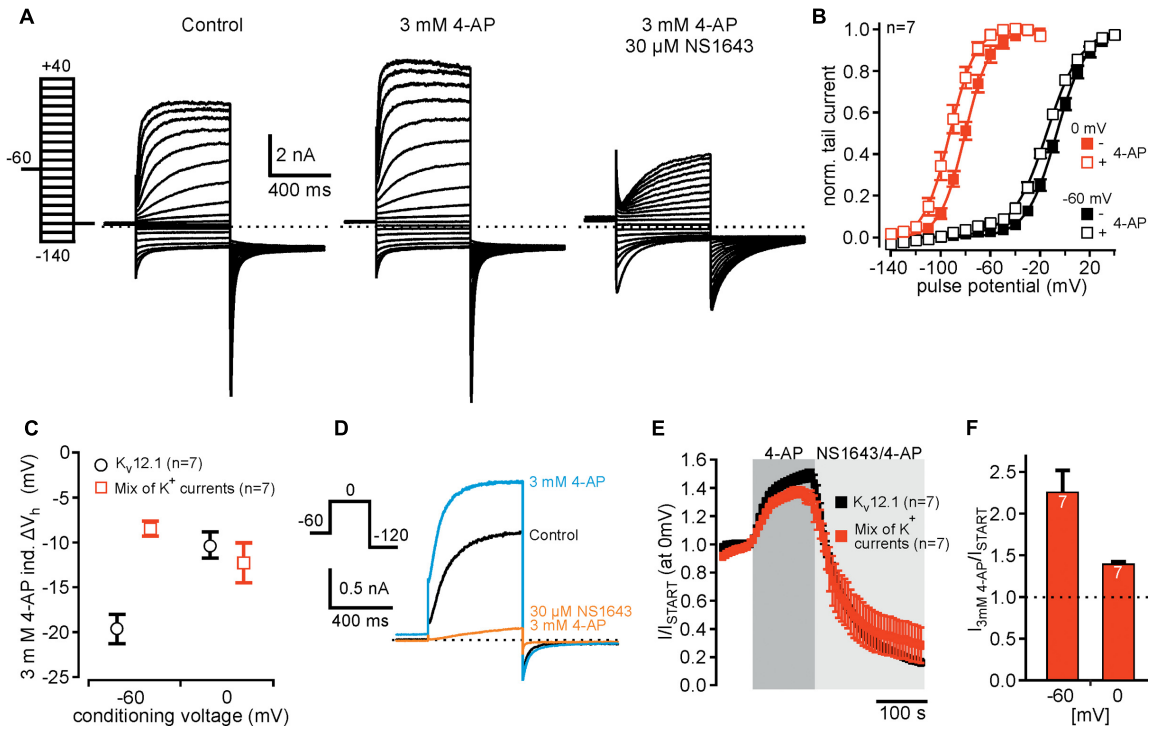

FIGURE 6 | Detection of $K_v12.1$ channel activity in cells expressing various K^+ currents. **(A)** Representative recordings of a CHO cell expressing different K^+ channel subunits ($K_v7.2$, $K_v7.3$, $K_v11.1$ and Kir2.1) together with $K_v12.1$ under control conditions (left), upon application of 3 mM 4-AP (middle) and of 4-AP together with 30 µM NS1643 (right) (voltage protocol as indicated). **(B)** Voltage dependence of whole cell currents in cells expressing the mix of K^+ channel subunits. V_h of whole cell currents was –6.7 ± 1.3 mV (black filled squares) after conditioning potential of –60 mV. When cells were held for 200 ms at a conditioning potential of 0 mV before the activation pulses, V_h of whole cell currents was –80.0 ± 2.1 mV (red filled squares). Application of 3 mM 4-AP shifted voltage dependence to hyperpolarized potentials for both conditioning potentials (open squares; graph displays Boltzmann fits to averaged data as solid lines). **(C)** 4-AP (3 mM)-induced shift of V_h to hyperpolarized potentials shown for cells expressing the mix of K^+ channels (red squares) in comparison to cells expressing only $K_v12.1$ (black circles). The 4-AP-induced shift of voltage dependence after conditioning voltage of –60 mV was smaller than in cells expressing only $K_v12.1$ channels. Data for $K_v12.1$ alone were derived from experiments also shown in **Figure 3E**. **(D,E)** Summary of time course and current amplitudes in cells expressing a mix of K^+ channels during during application of 4-AP and NS1643 (together with 4-AP). **(D)** Representative current traces recorded in cells expressing a mix of K^+ channels before (black), during application of 3 mM 4-AP (blue) and during application of 3 mM 4-AP together with 30 µM NS1643 (orange). **(E)** Averaged time course of current amplitudes upon application of 3 mM 4-AP and 30 µM NS1643 for CHO cells expressing $K_v12.1$ channels alone (black) and the mix of K^+ channels (red) (data obtained from recordings as presented in **D**). **(F)** Summarized 4-AP-induced potentiation of steady-state outward currents for cells expressing $K_v12.1$ channels together with a mix of neuronal K^+ channels. Data were derived from recordings as presented in **(D)**, and currents elicited at –60 mV and at 0 mV were analyzed.

Here, we focused on recombinant human $K_v12.1$ to identify distinct biophysical and pharmacological properties allowing for attribution of native currents to these channels.

Human $K_v12.1$ Channels Exhibit Mode Shift of Activation

Mode shift of activation was recently demonstrated for $K_v12.1$ channel isoforms of humans and zebrafish heterologously expressed in *Xenopus laevis* oocytes (Li et al., 2015; Dai and Zagotta, 2017). However, mode shift of these channels has not been characterized in mammalian cells in detail yet. We found that mode shift of human $K_v12.1$ was readily induced by depolarized holding potentials between −60 and 0 mV and that it manifested by slowed channel deactivation and a striking shift of voltage dependence to hyperpolarized potentials. Deceleration of deactivation is generally considered a biophysical hallmark of mode shift, as channels undergo additional (time-consuming) transitions from this "relaxed" (metastable) open state into deactivation (Bezanilla et al., 1982; Villalba-Galea et al., 2008; Corbin-Leftwich et al., 2016; Villalba-Galea, 2017). Similar to $K_v11.1$ (Tan et al., 2012) and zebrafish $K_v12.1$ (Dai and Zagotta, 2017), mode shift of human $K_v12.1$ channels manifested by a striking −60 mV shift of voltage dependence. Thus, mode shift-dependent hyperpolarizing shifts of voltage dependence were qualitatively and quantitatively comparable for these three ion channels. Of note, mode shift of $K_v12.1$ channels was readily induced using different voltage protocols, albeit the extent of the hyperpolarizing shift of activation potentials varied considerably with duration of hyperpolarized voltage steps. This demonstrated high sensitivity of $K_v12.1$ channels to the holding potential, but also highlighted that voltage dependence of native $K_v12.1$ currents might also vary with the used voltage protocols. In contrast to zebrafish $K_v12.1$ (Dai and Zagotta, 2017), activation of human $K_v12.1$ channels did not exhibit prominent double exponential kinetics that might indicate transition into a more stable open conformation. However, human $K_v11.1$ channels that

beyond doubt exhibit mode shift do not display such kinetics neither (Tan et al., 2012; Goodchild et al., 2015). This indicates that either kinetics were masked by channel inactivation, or transition was too fast in the human channel isoforms.

Time course of transition into the relaxed state varies considerably between channels requiring depolarization for minutes in Na_v (Bezanilla et al., 1982), seconds in *Shaker* (Olcese et al., 1997) and some hundreds of milliseconds in K_v11.1 channels (Piper et al., 2003). For human K_v12.1, we found that also some hundreds of milliseconds of conditioning depolarization was sufficient for significant alterations of voltage dependence and kinetics. Thus, time course of development of K_v12.1 mode shift was well in the range of that published for K_v11.1 channels (Piper et al., 2003). As K_v12.1 channels are highly sensitive to changes of the holding potential, voltage dependence of the channels strongly depends on the employed voltage protocols. In fact, such protocol differences could account for considerable variations in voltage dependence of K_v12.1 channels reported in different studies (V_h close to 0 mV in Shi et al., 1998; V_h of about −60 mV in Zou et al., 2003).

K_v12.1 Channels Are Activated by 4-AP, an Established K_v Channel Inhibitor

4-AP is a rather selective blocker of voltage-gated K^+ channels: At micromolar concentrations, it reversibly inhibits activity of K_v1 and K_v3 family members, but at higher concentrations (in the millimolar range) 4-AP also blocks other K_v channels (e.g., K_v11) (Gutman et al., 2005; Alexander et al., 2015). Thus, it was somewhat surprising to find that 4-AP activates K_v12.1 channels. As an early study mentioned potentiation of K_v12.3 through 4-AP without, however, showing any recordings (named rELK1; Engeland et al., 1998), such 4-AP sensitivity may constitute a general feature of the K_v12 family.

Earlier, it was shown that currents through K_v2.1 channels that are normally inhibited by 4-AP were potentiated by the substance, but only when K_v6.4 subunits were co-expressed (Stas et al., 2015). As K_v2.1 and K_v6.4 co-assemble into functional channels (reviewed in Bocksteins, 2016), this suggested that K_v6.4 largely determined altered 4-AP sensitivity of the resulting heteromeric channels. 4-AP suppressed closed state inactivation of K_v2.1/K_v6.4 resulting in exclusive current potentiation of currents through those heteromers (Stas et al., 2015). In contrast, K_v12.1 channels did not inactivate in our experiments, and thus 4-AP probably does not potentiate K_v12.1-mediated currents through a similar mechanism. As 4-AP, in contrast to K_v2.1/K_v6.4 heteromers, also modulated voltage dependence of K_v12.1, actions of 4-AP are probably even more complex for these channels. Interestingly, a recent study demonstrated 4-AP-dependent activation of K_v7.4 channels (Khammy et al., 2017) indicating that 4-AP-dependent activation of voltage-gated K^+ channels may constitute a more frequent phenomenon than expected. However, further work is needed to elucidate whether other members of the K_v channel superfamily also exhibit this special 4-AP sensitivity.

Yet, we do not know whether 4-AP directly activates K_v12.1 channels or whether an auxiliary subunit endogenously expressed in CHO cells confers 4-AP activation to K_v12.1. Unfortunately, at present nothing is known about physiologically relevant interaction partners of K_v12.1 channels. As K_v channels (with K_v2.1 as exception) normally do not form functional channels with members of other K_v families, heteromerization of K_v12.1 channels with another pore forming α subunit apart from K_v12.2 or K_v12.3 is quite unlikely (Zou et al., 2003). Accordingly, a mechanism as shown for K_v2.1 is rather implausible, and it is hard to imagine how a non-pore-forming auxiliary subunit could reverse 4-AP sensitivity from inhibition to activation. Furthermore, any endogenously expressed auxiliary subunit would need to be expressed at high abundance to saturate overexpressed K_v12.1 channels. Hence, a straightforward model proposes direct activation of K_v12.1 channels through 4-AP. However, we want to point-out that we cannot exclude indirect actions on the channels at the moment.

NS1643, a "Specific" Activator of K_v11 Channels, Inhibits K_v12.1

NS1643 is a well-characterized partial agonist of K_v11 channels that slows deactivation, increases tail-current amplitude, and shifts voltage dependence of activation to hyperpolarized potentials and voltage dependence of C-type inactivation to depolarized potentials (Casis et al., 2006; Hansen et al., 2006). At the same time, NS1643 exhibits weak antagonistic effects on K_v11 channels as evident by an attenuation of drug-induced current increase at higher concentrations (Casis et al., 2006; Schuster et al., 2011). K_v11.3 channels are even inhibited by higher concentrations of NS1643. For K_v12.1 channels, NS1643 accelerated deactivation, inhibited outward and tail currents and shifted voltage dependence of activation to depolarized potentials (c.f. **Figure 5**). Thus, NS1643 affected K_v11 and K_v12.1 channels exactly in opposite directions. Similar to K_v11.3 channels, NS1643 increased slope factor of voltage dependence of K_v12.1 channels, even though already at lower concentrations. This suggests that NS1643 similarly affects K_v11 and K_v12.1 channels, but antagonistic effects might dominate over activation for K_v12.1. In line, the concentration range of NS1643 effects was similar for these channel isoforms (Casis et al., 2006). However, so far we cannot tell whether NS1643 also exhibits weak agonistic effects on K_v12.1 channels or whether NS1643 binds to homologous regions in K_v11 and K_v12.1 channels.

Conclusion and Outlook

As pharmacological tools and appropriate mouse models are currently missing, identification of native K_v12.1-mediated currents critically depends on identification of unique biophysical and pharmacological properties. Indeed, native currents were successfully attributed to related K_v10 and K_v11 channels by exploiting their unique activation kinetics (c.f. Cole-Moore shift; e.g., Meyer and Heinemann, 1998) or exclusive Na^+ sensitivity and pharmacology (Hirdes et al., 2005, 2009; Hardman and Forsythe, 2009), respectively. Here, we present distinctive pharmacological properties, and straightforward experimental protocols that may be employed to isolate K_v12.1 channel activity in native tissue. As mode shift readily manifested in

cells expressing various neuronal K^+ currents, this experimental protocol may be used to demonstrate expression of channels with mode shift in native cell types. In neurons expressing various K^+ current components, such changes of voltage dependence may be easier to detect than associated changes of deactivation kinetics. Such experiments may not provide definite proof for K_v12 channel expression. However, expression of mode shift may be employed together with expression analyses, Na^+ sensitivity, activation through 4-AP and inhibition by NS1643 to narrow down (or exclude) contribution of $K_v12.1$ channels to whole cell currents. Identification of the combination of these properties would provide strong evidence for expression and thus potential physiological relevance of $K_v12.1$ channels.

MATERIALS AND METHODS

Cell Culture and Transfection

Chinese hamster ovary (CHO) dhFR$^-$ cells were maintained as previously reported (Leitner et al., 2016). Cells were kept in MEM Alpha Medium supplemented with 10% fetal calf serum (FCS) and 1% penicillin/streptomycin (pen/strep) (all Invitrogen GmbH, Darmstadt, Germany) in a humidified atmosphere at 5% CO_2 and 37°C. Transient transfection of cells was done with jetPEI transfection reagent (Polyplus Transfection, Illkirch, France). All experiments were performed 24–48 h after transfection at room temperature (22–25°C). The expression vectors used were: $K_v7.2$-pBK-CMV (gene: human KCNQ2; UniProt accession number: O43526), $K_v7.3$-pBK-CMV (human KCNQ3; O43525), $K_v7.4$-pBK-CMV (human KCNQ4; P56696) $K_v11.1$ (Erg1)-pcDNA3.1 (rat KCNH2; O08962), $K_v12.1$(Elk1)-pcDNA3.1-IRESeGFP (human KCNH8; Q96L42), Kir2.1-pBK-CMV (human KCNJ2; P63252), and pEGFP-C1 (Addgene, Teddington, United Kingdom). For recordings presented in **Figure 6** and Supplementary Figure 5, CHO cells were transiently transfected with identical amounts of plasmids encoding $K_v7.2$, $K_v7.3$, $K_v11.1$, $K_v12.1$, and Kir2.1 (0.6 μg of plasmid DNA for every subunit).

Electrophysiological Recordings

Electrophysiological recordings were performed in the whole cell configuration with an Axopatch 200B amplifier (Molecular Devices, Union City, CA, United States) or an HEKA EPC10 USB patch clamp amplifier HEKA (Elektronik, Lambrecht, Germany) in voltage-clamp mode (Leitner et al., 2011). All recordings were low-pass filtered at 2 kHz and sampled at 5 kHz. Currents were elicited by voltage protocols indicated in the figures. Dashed lines in representative recordings highlight zero current. Borosilicate glass patch pipettes (Sutter Instrument Company, Novato, CA, United States) were used with an open pipette resistance of 2–3 MΩ after back-filling with intracellular solution. Liquid junction potentials were not compensated (approximately −4 mV). Series resistance (R_s) typically was below 6 MΩ and compensated throughout the recordings (80–90%). Whole cell currents are presented normalized to the cell capacitance (current density; pA/pF) or as normalized to baseline current amplitude (I/I_{Start}). Extracellular solutions for most experiments contained (mM) 144 NaCl, 5.8 KCl, 1.3 $CaCl_2$, 0.9 $MgCl_2$, 0.7 NaH_2PO_4, 10 HEPES and 5.6 D-glucose, pH 7.4 (with NaOH), 305–310 mOsm/kg. In some experiments, NaCl in the extracellular solution was substituted by *N*-methyl-D-glucamine (NMDG; Sigma–Aldrich) (c.f. **Figure 2**). The standard intracellular solution contained (mM) 135 KCl, 2.41 $CaCl_2$ (100 nM free Ca^{2+}), 3.5 $MgCl_2$, 5 HEPES, 5 EGTA, 2.5 Na_2ATP, pH 7.3 (with KOH), 290–295 mOsm/kg (Wilke et al., 2014).

Substances

Tetraethylammonium (TEA, Sigma), NMDG (Sigma), 4-aminopyridine (≥99%; Sigma and Tocris Bioscience, Bristol, United Kingdom), 2-aminopyridine (2-AP; Sigma), 3-aminopyridine (3-AP; Sigma), 3,4-diaminopyridine (3,4-DAP; Sigma), 1,3-Bis-(2-hydroxy-5-trifluoromethyl-phenyl)-urea (NS 1643, Tocris), 10,10-*bis*(4-Pyridinylmethyl)-9(10*H*)-anthracenone dihydrochloride (XE991, Tocris), and *N*-[4-[[1-[2-(6-Methyl-2-pyridinyl)ethyl]-4-piperidinyl]carbonyl]phenyl] methanesulfonamide dihydrochloride (E-4031, Tocris) were diluted in extracellular solution to concentrations indicated in "Results." All substances were applied locally via a glass capillary through a custom-made application system.

Note on 4-AP Solutions

4-AP did not significantly change the pH of the extracellular solution at concentrations below 3 mM. After dilution of the substance, pH of the extracellular solution containing 5 mM or 10 mM 4-AP typically was about 8.1 or 9.0, respectively. As indicated in "Results," in some experiments the pH of solutions containing 5 and 10 mM 4-AP was adjusted to 7.4 after dilution of 4-AP. At the concentration applied in the present study (3 mM), isomeric aminopyridines did not change pH of the extracellular solution (c.f. **Figure 4**).

Data Analysis

Patch clamp recordings were analyzed with PatchMaster (HEKA) and IgorPro (Wavemetrics, Lake Oswego, OR, United States). Voltage dependence of activation was derived from tail current amplitudes using voltage protocols indicated: Tail currents were fitted with a two-state Boltzmann function with $I = I_{min} + (I_{max} - I_{min})/(1 + exp((V - V_h)/s))$, where I is current, V is the membrane voltage, V_h is the voltage at half maximal activation, and s describes the steepness of the curve. Results are shown as conductance-voltage curves, obtained by normalizing to $(I_{max} - I_{min})$, obtained from fits to data of individual experiments. Time constants of deactivation were derived from double-exponential fits to deactivating current components at indicated potentials. For dose-response relations, current potentiation at 0 mV (normalized to baseline) was fitted to a Hill equation with $I/I_b = I_b + (I_{max} - I_b)/(1 + (EC_{50}/[S])^{n_H})$, where I is the (normalized) current, I_b and I_{max} denote minimal and maximal currents at low and high drug concentrations, EC_{50} is the concentration at the half maximal effect, [S] is the drug concentration and n_H is the Hill coefficient (Leitner et al., 2012).

Statistical Analysis

Isolated cells under investigation were randomly assigned to different treatment groups. Data recordings and analysis for experiments presented were not performed in a blinded manner. For some experiments, single recordings were normalized to base line values individually to account for baseline variations between cells. Statistical analysis was performed using two-tailed Student's *t*-test/Wilcoxon–Mann–Whitney test, and when appropriate comparisons between multiple groups were performed with ANOVA followed by Dunnett test. Significance was assigned at $P \leq 0.05$ ($^{*}P \leq 0.05$, $^{**}P \leq 0.01$, $^{***}P \leq 0.001$). Data subjected to statistical analysis have n over 5 per group and data are presented as mean ± SEM. In electrophysiological experiments, n represents the number of individual cells and accordingly the number of independent experiments (no pseudo-replication).

AUTHOR CONTRIBUTIONS

MD, SE, BW, and ML planned and performed the experiments and analyzed the data. ML conceived study, designed the experiments, and wrote the paper together with MD. All authors revised and approved the final version of the manuscript. All experiments were conducted at the Institute of Physiology and Pathophysiology at the Philipps-University Marburg (Germany).

FUNDING

This work was funded by Research Grants of the University Medical Center Giessen und Marburg (UKGM 17/2013; UKGM 13/2016 to ML) and by the German Research Foundation (DFG Priority Program 1608: "Ultrafast and temporally precise information processing: normal and dysfunctional hearing," [LE 3600/1-1 to ML]).

ACKNOWLEDGMENTS

The authors acknowledge the kind gift of plasmids for K_V7 (KCNQ) channels from Dr. T. Jentsch, $K_V12.1$ (Elk) from Dr. T. Jegla, and $K_V11.1$ (Erg) from Dr. C. Bauer. They thank Olga Ebers and Neslihan Özen for superb technical assistance and Dr. Dominik Oliver (Marburg) for helpful comments and discussion.

SUPPLEMENTARY MATERIAL

The Supplementary Material for this article can be found online at: https://www.frontiersin.org/articles/10.3389/fnmol.2018.00011/full#supplementary-material

REFERENCES

Alexander, S. P., Catterall, W. A., Kelly, E., Marrion, N., Peters, J. A., Benson, H. E., et al. (2015). The concise guide to PHARMACOLOGY 2015/16: voltage-gated ion channels. *Br. J. Pharmacol.* 172, 5904–5941. doi: 10.1111/bph.13349

Bauer, C. K., and Schwarz, J. R. (2001). Physiology of EAG K+ channels. *J. Membr. Biol.* 182, 1–15. doi: 10.1007/s00232-001-0031-3

Bezanilla, F., Taylor, R. E., and Fernandez, J. M. (1982). Distribution and kinetics of membrane dielectric polarization. 1. Long-term inactivation of gating currents. *J. Gen. Physiol.* 79, 21–40. doi: 10.1085/jgp.79.1.21

Bocksteins, E. (2016). Kv5, Kv6, Kv8, and Kv9 subunits: no simple silent bystanders. *J. Gen. Physiol.* 147, 105–125. doi: 10.1085/jgp.201511507

Bruening-Wright, A., and Larsson, H. P. (2007). Slow conformational changes of the voltage sensor during the mode shift in hyperpolarization-activated cyclic-nucleotide-gated channels. *J. Neurosci.* 27, 270–278. doi: 10.1523/JNEUROSCI.3801-06.2007

Casis, O., Olesen, S. P., and Sanguinetti, M. C. (2006). Mechanism of action of a novel human ether-a-go-go-related gene channel activator. *Mol. Pharmacol.* 69, 658–665. doi: 10.1124/mol.105.019943

Corbin-Leftwich, A., Mossadeq, S. M., Ha, J., Ruchala, I., Le, A. H., and Villalba-Galea, C. A. (2016). Retigabine holds KV7 channels open and stabilizes the resting potential. *J. Gen. Physiol.* 147, 229–241. doi: 10.1085/jgp.201511517

Curran, M. E., Splawski, I., Timothy, K. W., Vincent, G. M., Green, E. D., and Keating, M. T. (1995). A molecular basis for cardiac arrhythmia: HERG mutations cause long QT syndrome. *Cell* 80, 795–803. doi: 10.1016/0092-8674(95)90358-5

Dai, G., and Zagotta, W. N. (2017). Molecular mechanism of voltage-dependent potentiation of KCNH potassium channels. *Elife* 6:e26355. doi: 10.7554/eLife.26355

Engeland, B., Neu, A., Ludwig, J., Roeper, J., and Pongs, O. (1998). Cloning and functional expression of rat ether-a-go-go-like K+ channel genes. *J. Physiol.* 513(Pt 3), 647–654.

Goodchild, S. J., Macdonald, L. C., and Fedida, D. (2015). Sequence of gating charge movement and pore gating in HERG activation and deactivation pathways. *Biophys. J.* 108, 1435–1447. doi: 10.1016/j.bpj.2015.02.014

Gutman, G. A., Chandy, K. G., Grissmer, S., Lazdunski, M., Mckinnon, D., Pardo, L. A., et al. (2005). International union of pharmacology. LIII. Nomenclature and molecular relationships of voltage-gated potassium channels. *Pharmacol. Rev.* 57, 473–508. doi: 10.1124/pr.57.4.10

Hadley, J. K., Noda, M., Selyanko, A. A., Wood, I. C., Abogadie, F. C., and Brown, D. A. (2000). Differential tetraethylammonium sensitivity of KCNQ1-4 potassium channels. *Br. J. Pharmacol.* 129, 413–415. doi: 10.1038/sj.bjp.0703086

Hansen, R. S., Diness, T. G., Christ, T., Demnitz, J., Ravens, U., Olesen, S. P., et al. (2006). Activation of human ether-a-go-go-related gene potassium channels by the diphenylurea 1,3-bis-(2-hydroxy-5-trifluoromethyl-phenyl)-urea (NS1643). *Mol. Pharmacol.* 69, 266–277.

Hardman, R. M., and Forsythe, I. D. (2009). Ether-a-go-go-related gene K+ channels contribute to threshold excitability of mouse auditory brainstem neurons. *J. Physiol.* 587, 2487–2497. doi: 10.1113/jphysiol.2009.170548

Hirdes, W., Napp, N., Wulfsen, I., Schweizer, M., Schwarz, J. R., and Bauer, C. K. (2009). Erg K+ currents modulate excitability in mouse mitral/tufted neurons. *Pflugers. Arch.* 459, 55–70. doi: 10.1007/s00424-009-0709-4

Hirdes, W., Schweizer, M., Schuricht, K. S., Guddat, S. S., Wulfsen, I., Bauer, C. K., et al. (2005). Fast erg K+ currents in rat embryonic serotonergic neurons. *J. Physiol.* 564, 33–49. doi: 10.1113/jphysiol.2004.082123

Ji, H., Tucker, K. R., Putzier, I., Huertas, M. A., Horn, J. P., Canavier, C. C., et al. (2012). Functional characterization of ether-a-go-go-related gene potassium channels in midbrain dopamine neurons - implications for a role in depolarization block. *Eur. J. Neurosci.* 36, 2906–2916. doi: 10.1111/j.1460-9568.2012.08190.x

Kazmierczak, M., Zhang, X., Chen, B., Mulkey, D. K., Shi, Y., Wagner, P. G., et al. (2013). External pH modulates EAG superfamily K+ channels through EAG-specific acidic residues in the voltage sensor. *J. Gen. Physiol.* 141, 721–735. doi: 10.1085/jgp.201210938

Khammy, M. M., Kim, S., Bentzen, B. H., Lee, S., Choi, I., Aalkjaer, C., et al. (2017). 4-aminopyridine: a pan Kv channel inhibitor that enhances Kv7.4 currents and inhibits noradrenaline-mediated contraction of rat mesenteric small arteries. *Br. J. Pharmacol.* doi: 10.1111/bph.14097 [Epub ahead of print].

Kortum, F., Caputo, V., Bauer, C. K., Stella, L., Ciolfi, A., Alawi, M., et al. (2015). Mutations in KCNH1 and ATP6V1B2 cause zimmermann-laband syndrome. *Nat. Genet.* 47, 661–667. doi: 10.1038/ng.3282

Leitner, M. G., Feuer, A., Ebers, O., Schreiber, D. N., Halaszovich, C. R., and Oliver, D. (2012). Restoration of ion channel function in deafness-causing KCNQ4 mutants by synthetic channel openers. *Br. J. Pharmacol.* 165, 2244–2259. doi: 10.1111/j.1476-5381.2011.01697.x

Leitner, M. G., Halaszovich, C. R., and Oliver, D. (2011). Aminoglycosides inhibit KCNQ4 channels in cochlear outer hair cells via depletion of phosphatidylinositol(4,5)bisphosphate. *Mol. Pharmacol.* 79, 51–60. doi: 10.1124/mol.110.068130

Leitner, M. G., Michel, N., Behrendt, M., Dierich, M., Dembla, S., Wilke, B. U., et al. (2016). Direct modulation of TRPM4 and TRPM3 channels by the phospholipase C inhibitor U73122. *Br. J. Pharmacol.* 173, 2555–2569. doi: 10.1111/bph.13538

Li, X., Anishkin, A., Liu, H., Van Rossum, D. B., Chintapalli, S. V., Sassic, J. K., et al. (2015). Bimodal regulation of an Elk subfamily K+ channel by phosphatidylinositol 4,5-bisphosphate. *J. Gen. Physiol.* 146, 357–374. doi: 10.1085/jgp.201511491

Mannikko, R., Pandey, S., Larsson, H. P., and Elinder, F. (2005). Hysteresis in the voltage dependence of HCN channels: conversion between two modes affects pacemaker properties. *J. Gen. Physiol.* 125, 305–326. doi: 10.1085/jgp.200409130

Marcotti, W., Johnson, S. L., Holley, M. C., and Kros, C. J. (2003). Developmental changes in the expression of potassium currents of embryonic, neonatal and mature mouse inner hair cells. *J. Physiol.* 548, 383–400. doi: 10.1113/jphysiol.2002.034801

Meyer, R., and Heinemann, S. H. (1998). Characterization of an eag-like potassium channel in human neuroblastoma cells. *J. Physiol.* 508(Pt 1), 49–56. doi: 10.1111/j.1469-7793.1998.049br.x

Miyake, A., Mochizuki, S., Yokoi, H., Kohda, M., and Furuichi, K. (1999). New ether-a-go-go K(+) channel family members localized in human telencephalon. *J. Biol. Chem.* 274, 25018–25025. doi: 10.1074/jbc.274.35.25018

Miyake, A., Takahashi, S., Nakamura, Y., Inamura, K., Matsumoto, S., Mochizuki, S., et al. (2009). Disruption of the ether-a-go-go K+ channel gene BEC1/KCNH3 enhances cognitive function. *J. Neurosci.* 29, 14637–14645. doi: 10.1523/JNEUROSCI.0901-09.2009

Numaguchi, H., Johnson, J. P. Jr., Petersen, C. I., and Balser, J. R. (2000). A sensitive mechanism for cation modulation of potassium current. *Nat. Neurosci.* 3, 429–430. doi: 10.1038/74793

Olcese, R., Latorre, R., Toro, L., Bezanilla, F., and Stefani, E. (1997). Correlation between charge movement and ionic current during slow inactivation in Shaker K+ channels. *J. Gen. Physiol.* 110, 579–589. doi: 10.1085/jgp.110.5.579

Pardo, L. A., and Stuhmer, W. (2014). The roles of K(+) channels in cancer. *Nat. Rev. Cancer* 14, 39–48. doi: 10.1038/nrc3635

Piper, D. R., Varghese, A., Sanguinetti, M. C., and Tristani-Firouzi, M. (2003). Gating currents associated with intramembrane charge displacement in HERG potassium channels. *Proc. Natl. Acad. Sci. U.S.A.* 100, 10534–10539. doi: 10.1073/pnas.1832721100

Ridley, J. M., Milnes, J. T., Zhang, Y. H., Witchel, H. J., and Hancox, J. C. (2003). Inhibition of HERG K+ current and prolongation of the guinea-pig ventricular action potential by 4-aminopyridine. *J. Physiol.* 549, 667–672. doi: 10.1113/jphysiol.2003.043976

Robertson, B. E., and Nelson, M. T. (1994). Aminopyridine inhibition and voltage dependence of K+ currents in smooth muscle cells from cerebral arteries. *Am. J. Physiol.* 267, C1589–C1597. doi: 10.1152/ajpcell.1994.267.6.C1589

Saganich, M. J., Machado, E., and Rudy, B. (2001). Differential expression of genes encoding subthreshold-operating voltage-gated K+ channels in brain. *J. Neurosci.* 21, 4609–4624.

Sanchez, A., Urrego, D., and Pardo, L. A. (2016). Cyclic expression of the voltage-gated potassium channel KV10.1 promotes disassembly of the primary cilium. *EMBO Rep.* 17, 708–723. doi: 10.15252/embr.201541082

Sanguinetti, M. C., Jiang, C., Curran, M. E., and Keating, M. T. (1995). A mechanistic link between an inherited and an acquired cardiac arrhythmia: HERG encodes the IKr potassium channel. *Cell* 81, 299–307. doi: 10.1016/0092-8674(95)90340-2

Schuster, A. M., Glassmeier, G., and Bauer, C. K. (2011). Strong activation of ether-a-go-go-related gene 1 K+ channel isoforms by NS1643 in human embryonic kidney 293 and Chinese hamster ovary cells. *Mol. Pharmacol.* 80, 930–942. doi: 10.1124/mol.111.071621

Sedehizadeh, S., Keogh, M., and Maddison, P. (2012). The use of aminopyridines in neurological disorders. *Clin. Neuropharmacol.* 35, 191–200. doi: 10.1097/WNF.0b013e31825a68c5

Shi, W., Wang, H. S., Pan, Z., Wymore, R. S., Cohen, I. S., Mckinnon, D., et al. (1998). Cloning of a mammalian elk potassium channel gene and EAG mRNA distribution in rat sympathetic ganglia. *J. Physiol.* 511(Pt 3), 675–682.

Simons, C., Rash, L. D., Crawford, J., Ma, L., Cristofori-Armstrong, B., Miller, D., et al. (2015). Mutations in the voltage-gated potassium channel gene KCNH1 cause Temple-Baraitser syndrome and epilepsy. *Nat. Genet.* 47, 73–77. doi: 10.1038/ng.3153

Stas, J. I., Bocksteins, E., Labro, A. J., and Snyders, D. J. (2015). Modulation of closed-state inactivation in Kv2.1/Kv6.4 heterotetramers as mechanism for 4-AP induced potentiation. *PLOS ONE* 10:e0141349. doi: 10.1371/journal.pone.0141349

Strupp, M., Teufel, J., Zwergal, A., Schniepp, R., Khodakhah, K., and Feil, K. (2017). Aminopyridines for the treatment of neurologic disorders. *Neurol. Clin. Pract.* 7, 65–76. doi: 10.1212/CPJ.0000000000000321

Sturm, P., Wimmers, S., Schwarz, J. R., and Bauer, C. K. (2005). Extracellular potassium effects are conserved within the rat erg K+ channel family. *J. Physiol.* 564, 329–345. doi: 10.1113/jphysiol.2004.078840

Tan, P. S., Perry, M. D., Ng, C. A., Vandenberg, J. I., and Hill, A. P. (2012). Voltage-sensing domain mode shift is coupled to the activation gate by the N-terminal tail of hERG channels. *J. Gen. Physiol.* 140, 293–306. doi: 10.1085/jgp.201110761

Tilegenova, C., Cortes, D. M., and Cuello, L. G. (2017). Hysteresis of KcsA potassium channel's activation- deactivation gating is caused by structural changes at the channel's selectivity filter. *Proc. Natl. Acad. Sci. U.S.A.* 114, 3234–3239. doi: 10.1073/pnas.1618101114

Trudeau, M. C., Titus, S. A., Branchaw, J. L., Ganetzky, B., and Robertson, G. A. (1999). Functional analysis of a mouse brain Elk-type K+ channel. *J. Neurosci.* 19, 2906–2918.

Trudeau, M. C., Warmke, J. W., Ganetzky, B., and Robertson, G. A. (1995). HERG, a human inward rectifier in the voltage-gated potassium channel family. *Science* 269, 92–95. doi: 10.1126/science.7604285

Urrego, D., Movsisyan, N., Ufartes, R., and Pardo, L. A. (2016). Periodic expression of Kv10.1 driven by pRb/E2F1 contributes to G2/M progression of cancer and non-transformed cells. *Cell Cycle* 15, 799–811. doi: 10.1080/15384101.2016.1138187

Villalba-Galea, C. A. (2017). Hysteresis in voltage-gated channels. *Channels* 11, 140–155. doi: 10.1080/19336950.2016.1243190

Villalba-Galea, C. A., Sandtner, W., Starace, D. M., and Bezanilla, F. (2008). S4-based voltage sensors have three major conformations. *Proc. Natl. Acad. Sci. U.S.A.* 105, 17600–17607. doi: 10.1073/pnas.0807387105

Wang, H. S., Pan, Z., Shi, W., Brown, B. S., Wymore, R. S., Cohen, I. S., et al. (1998). KCNQ2 and KCNQ3 potassium channel subunits: molecular correlates of the M-channel. *Science* 282, 1890–1893. doi: 10.1126/science.282.5395.1890

Wilke, B. U., Lindner, M., Greifenberg, L., Albus, A., Kronimus, Y., Bunemann, M., et al. (2014). Diacylglycerol mediates regulation of TASK potassium channels by Gq-coupled receptors. *Nat. Commun.* 5:5540. doi: 10.1038/ncomms6540

Zhang, X., Bertaso, F., Yoo, J. W., Baumgartel, K., Clancy, S. M., Lee, V., et al. (2010). Deletion of the potassium channel Kv12.2 causes hippocampal hyperexcitability and epilepsy. *Nat. Neurosci.* 13, 1056–1058. doi: 10.1038/nn.2610

Zou, A., Lin, Z., Humble, M., Creech, C. D., Wagoner, P. K., Krafte, D., et al. (2003). Distribution and functional properties of human KCNH8 (Elk1) potassium channels. *Am. J. Physiol. Cell Physiol.* 285, C1356–C1366. doi: 10.1152/ajpcell.00179.2003

Conflict of Interest Statement: The authors declare that the research was conducted in the absence of any commercial or financial relationships that could be construed as a potential conflict of interest.

Copyright © 2018 Dierich, Evers, Wilke and Leitner. This is an open-access article distributed under the terms of the Creative Commons Attribution License (CC BY). The use, distribution or reproduction in other forums is permitted, provided the original author(s) and the copyright owner are credited and that the original publication in this journal is cited, in accordance with accepted academic practice. No use, distribution or reproduction is permitted which does not comply with these terms.